Journal of Magnetism and Magnetic Materials 401 (2016) 812–815

Contents lists available at ScienceDirect

Journal of Magnetism and Magnetic Materials

journal homepage: www.elsevier.com/locate/jmmm

Magnetic properties and magnetocaloric response of mixed valence $La_{2/3}Ba_{1/3}Mn_{1-x}Fe_xO_3$ manganites

I. Betancourt [a,*], L. Lopez Maldonado [b], J.T. Elizalde Galindo [b]

[a] Departamento de Materiales Metálicos y Cerámicos, Instituto de Investigaciones en Materiales, Universidad Nacional Autónoma de México, México D.F. 04510, México

[b] Instituto de Ingeniería y Tecnología, Universidad Autónoma de Ciudad Juárez, Ciudad Juárez 32310, México

ARTICLE INFO

Article history:
Received 25 August 2015
Received in revised form
9 October 2015
Accepted 31 October 2015
Available online 2 November 2015

Keywords:
Mixed valence manganites
Magnetocaloric effect
Curie temperature
Magnetic entropy

ABSTRACT

Polycrystalline manganites of composition $La_{2/3}Ba_{1/3}Mn_{1-x}Fe_xO_3$ ($x=0.0$–0.10) were obtained by the Pechini method. Magnetic properties exhibited a marked dependence with Fe content, showing significant reductions for the saturation magnetization and the Curie temperature. The magnetocaloric effect was quantified for all the samples by means of the magnetic entropy variations, which showed a maximum of 1.46 J/kgK for Fe content of $x=0.025$. Results were interpreted on the basis of a deleterious effect on the double exchange interaction provoked by the presence of Fe^{3+} ions within the crystal structure.

1. Introduction

Mixed valence perovskites based on Mn oxides (also known as manganites) with general formula $A_{1-x}B_xMnO_3$ (where A is a trivalent cation like La, Pr, Nd, Sm, Gd, Ho or Y, whereas B stands for a divalent cation like Ca, Sr, Ba, Pb) have been extensively studied since the 1950's because of their richness in transport and magnetic properties, including a variety of couplings between charge, spin, orbital and vibrational degrees of freedom, together with features of technological interest like colossal magnetoresistance, magnetocaloric effect and unconventional insulator-metal transitions [1–5]. From a fundamental viewpoint, the complex electronic behavior of mixed valence perovskites relies to a significant extent on the double exchange (DE) interaction, which is afforded by the conversion of Mn^{3+} into proportional numbers of Mn^{4+} by doping the original $AMnO_3$ compound with divalent-type B ions. On the basis of the electronic configuration of Mn^{3+} ($t_{2g}^3 e_g^1$) and Mn^{4+} ($t_{2g}^3 e_g^0$), it can be elucidated that the presence of Mn^{4+} ions allow the hopping of e_g electrons of Mn^{3+} to neighboring Mn^{4+} through DE interaction, which in turn mediates ferromagnetic ordering and conduction. In particular, La-based manganites have elicited an intense interest of investigation due to the very rich phase diagram reported for $La_{1-x}Sr_xMnO_3$ and $La_{1-x}Ca_xMnO_3$ systems, characterized by multi-phase transitions including paramagnetic insulator, paramagnetic metallic, spin-canted insulator, ferromagnetic insulator, ferromagnetic metallic, antiferromagnetic metallic, charge-ordered and canted antiferromagnetic states, together with ample variations of the associated critical temperatures [1,5,6 and references therein]. Another important perovskite system is $La_{1-x}Ba_xMnO_3$, which also exhibit a complex interplay between chemical composition, structural variations, heat treatments and electronic properties [7–12].

The magnetocaloric effect (MCE), which refers to the isothermal magnetic entropy change (accompanied by an adiabatic temperature variation) of a magnetic material under the application of an external magnetic field, has been studied extensively in LaSr- and LaBa-based manganites because of the possibility for developing room temperature magnetic refrigeration technology based on their competitive cost of production, chemical stability and easy tailoring of magnetic properties [3]. Although a significant number of compositional variations have been explored for LaBa-, LaCa- and LaSr-based manganites, reports concerning the effect of the systematic variation of Fe content on the magnetic properties and MCE in LaBa-based manganites are not available [3,13]. In this work, we present a systematic study on the magnetic properties, including MCE, of $La_{2/3}Ba_{1/3}Mn_{1-x}Fe_xO_3$ ($x=0.0$–0.10) manganites obtained by Pechini method. The selected La:Ba ratio lies within the ferromagnetic zone (according to the phase diagram for $La_{1-x}Ba_xMnO_3$ manganites [14]) which affords to establish the correlation between magnetic properties and the valence state of the constituent transition-metal atoms, without additional

* Corresponding author.
E-mail address: israelb@unam.mx (I. Betancourt).

http://dx.doi.org/10.1016/j.jmmm.2015.10.137
0304-8853/

effects between different competing magnetic phases.

2. Materials and methods

The manganites series $La_{2/3}Ba_{1/3}Mn_{1-x}Fe_xO_3$ ($x=0.0$, 0.025, 0.050, 0.075, 0.10) were synthesized by means of the Pechini method [15–17]. This method affords the formation of small particles with narrow size distribution via a modified sol–gel synthetic route, with reaction temperatures below 1000 °C. The following precursors were used: $La(NO_3)_3 \cdot 6H_2O$ (Fluka ≥ 99.0%), $Mn(NO_3)_2 \cdot 6H_2O$ (AlfaAesar ≥ 99.98%), $Ba(NO_3)_2$ (Aldrich ≥ 99.99%), and $Fe(NO_3)_3 \cdot 9H_2O$ (Mallinckrodt ≥ 99.0%). The initial solution was prepared by mixing distilled water and the nitrates (properly weighed according to the specific composition), citric acid and ethyleneglycol. The mixture was then dried at 65 °C for 12 h. At this point, the resultant dried polymer was ground for a calcination treatment of 900 °C for 10 h in a muffla (Thermolyne 47900). A subsequent sinterization at 1100 °C for 48 h was carried out on pellets obtained from repulverized samples. The microstructure features were characterized by means of XRD analysis with Cu-K_α radiation and by Scanning Electron Microscopy (SEM) in a Leica-Cambridge equipment operating at 20 kV and coupled with EDS detector. Magnetic properties were determined by means of a Quantum Design Versalab system over a temperature interval ranging from 50 to 350 K. The MCE was quantified by means of the magnetic entropy variation $-\Delta S_M$, which was determined across the compositional series by numerical integration of the Maxwell relation based on isothermal magnetization curves measured in a range of temperatures around the Curie transition as follows

$$-\Delta S_M(T) = \int_o^{H_{max}} \left(\frac{\partial M}{\partial T}\right)_B dH \quad (1)$$

where M is the magnetization, T corresponds to the absolute temperature and H to the external applied field.

3. Results

XRD diffractograms for the manganite series $La_{2/3}Ba_{1/3}Mn_{1-x}Fe_xO_3$ ($x=0.0$–0.10) are shown in Fig. 1, for which all the diffracting planes between $2\theta=20-80°$ correspond to the perovskite

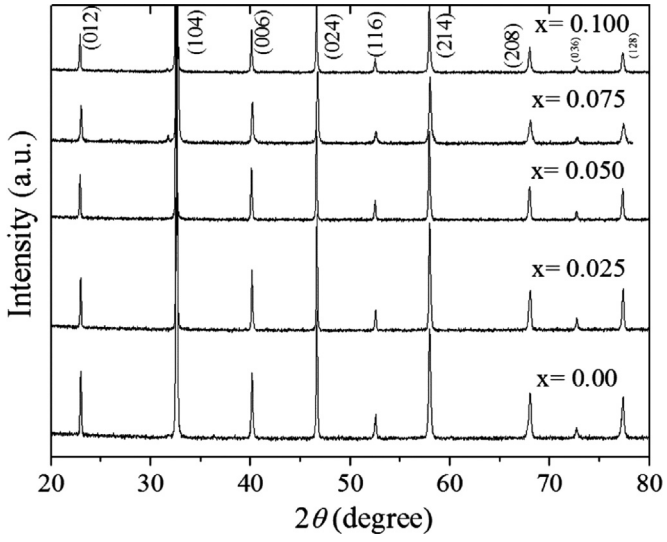

Fig. 1. XRD diffractograms for the manganites series $La_{2/3}Ba_{1/3}Mn_{1-x}Fe_xO_3$ ($x=0.0$–0.10).

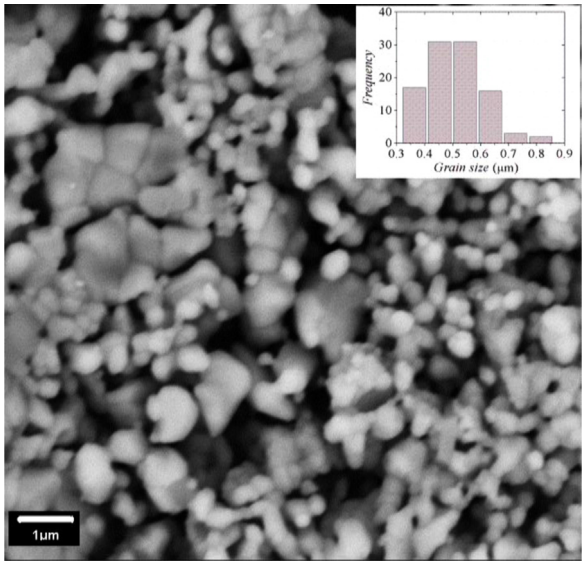

Fig. 2. SEM micrograph (secondary electrons) showing the polycrystalline character for the $La_{2/3}Ba_{1/3}Mn_{0.975}Fe_{0.025}O_3$ sample at a magnification of 50 k. The grain size distribution is shown as inset.

$La_{2/3}Ba_{1/3}MnO_3$ with rhombohedral distortion ($R\bar{3}c$ space group), according to ICDD file 01–072–8053. No secondary phases were observed.

SEM observations manifest the formation of a homogeneously dispersed polycrystalline distribution for all the samples, as illustrated in Fig. 2 for the selected composition $La_{2/3}Ba_{1/3}Mn_{0.975}Fe_{0.025}O_3$, displaying polyhedral grains with mean diameter below 1.0 μm, (according to the grain size distribution, included as inset), as well as porosity and aggregated grains.

Concerning magnetic properties, hysteresis loops at room temperature for the $La_{2/3}Ba_{1/3}Mn_{1-x}Fe_xO_3$ series are shown in Fig. 3. A marked deleterious effect on the magnetic response is observed for increasing Fe content x: From ferromagnetic behavior at $x=0.0$ and 0.025, to paramagnetic response for $x \geq 0.050$, together with a noticeable decrease in the magnetization saturation M_s, from 47 emu/g to 29 emu/g.

Complementary, thermomagnetic $M(T)$ curves measured under an applied field of 50 Oe are displayed in Fig. 4. A usual increasing behavior of magnetization with decreasing temperature is manifested for all the samples, as a result of the transition from paramagnetic to ferromagnetic ordering at the Curie temperature, T_c. For $x > 0.00$, only a single transition is visible, consistent with the

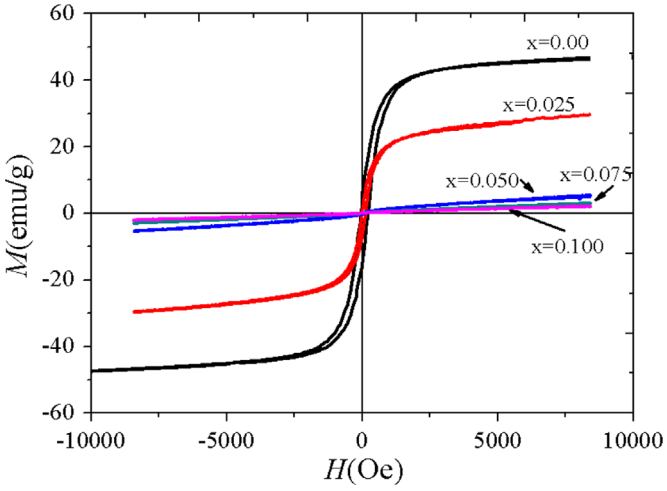

Fig. 3. Hysteresis M–H loops for the $La_{2/3}Ba_{1/3}Mn_{1-x}Fe_xO_3$ manganites series.

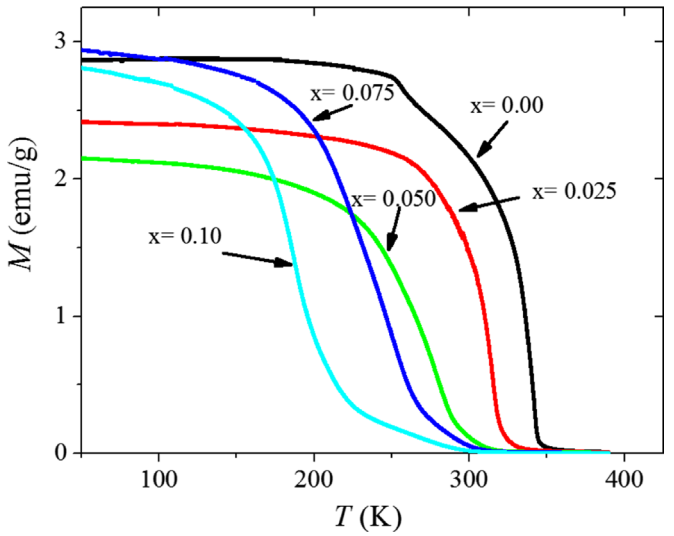

Fig. 4. Thermomagnetic curves for the $La_{2/3}Ba_{1/3}Mn_{1-x}Fe_xO_3$ manganites series.

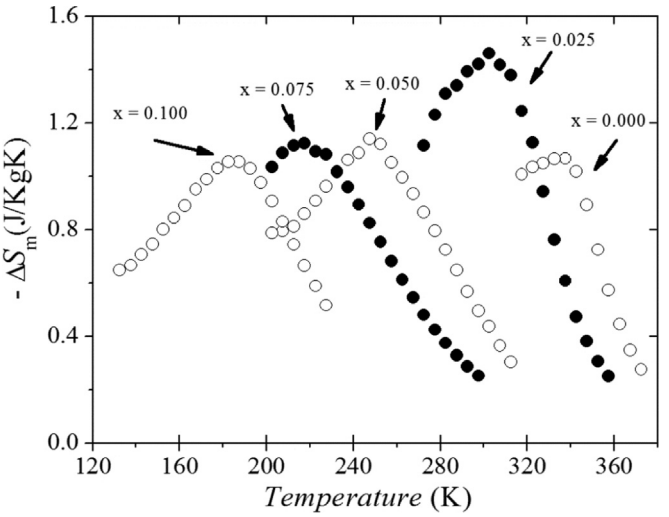

Fig. 6. Magnetic entropy variation $-\Delta S_m$ for the $La_{2/3}Ba_{1/3}Mn_{1-x}Fe_xO_3$ manganites series. ΔS_m^{peak} of each composition coincides with its T_c transition.

phase distribution indicated by XRD analysis (Fig. 1), whereas the initial $La_{2/3}Ba_{1/3}MnO_3$ sample ($x=0.0$) exhibits a subtle step around $T=255$ K, which can be associated with a minor secondary phase present in a volume fraction below the detection limit of the XRD technique (~4%). This additional phase probably correspond to an oxygen excessive $La_{1-x}Ba_xMnO_{3+\delta}$, which has been reported as a secondary phase alongside stoichiometric $La_{1-x}Ba_xMnO_3$ manganites [7,9]. The Curie transition for this off-stoichiometric $La_{1-x}Ba_xMnO_{3+\delta}$ phase depends on Ba and O content but, for $x=0.33$, the Curie transition occurs around 250 K [7,9].

Curie temperatures for all the samples was determined at the inflection point of each $M(T)$ plot (Fig. 5). A decreasing tendency for T_c is clearly manifested for augmenting Fe concentration, with T_c values above room temperature only for $x \leq 0.025$, which is consistent with the M–H loops recorded in Fig. 3.

Magnetic entropy variation $-\Delta S_m$ curves as a function of temperature T (with a fixed $\Delta H=2.5$ T) are shown in Fig. 6. Peak values $-\Delta S_m^{peak}$ for each composition coincide with T_c transition, showing an initial increase from $-\Delta S_m^{peak}=1.06$ J/kgK ($x=0.0$) to 1.46 J/kgK ($x=0.025$) and subsequent reduced values (≤ 1.14 J/kgK) for $x \geq 0.050$. This behavior can be ascribed to the change of the slope of $M(T)$ curves (Fig. 4) at the Curie transition, which follows the same tendency as $-\Delta S_m$ curves, since according to Eq. (1), ΔS_m depends on the slope $\partial M/\partial T$ of $M(T)$ at T_c. The maximum of $-\Delta S_m^{peak}$ (1.46 J/kgK) for the $La_{2/3}Ba_{1/3}M_{0.975}Fe_{0.025}O_3$ manganite favorably compares with their $La_{0.7}Sr_{0.3}(MnFe)O_3$ counterpart, for which entropy variations lower than -1.40 J/kgK (for same $\Delta H=2.5$ T) have been reported [18].

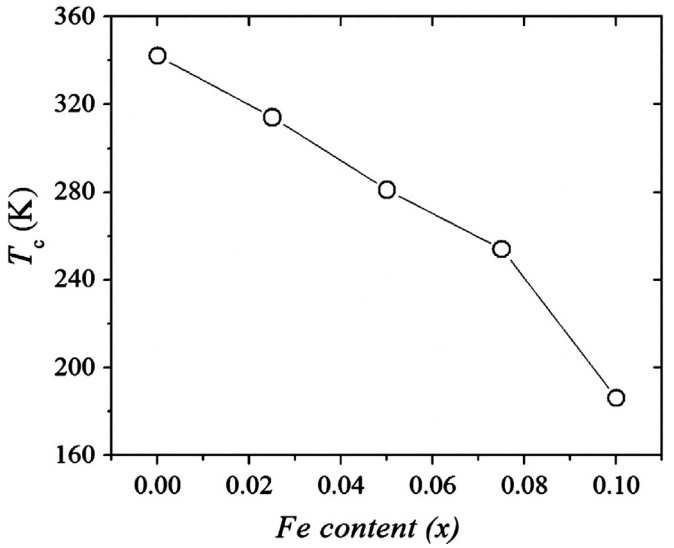

Fig. 5. Curie temperature T_c as a function of Fe content x for the $La_{2/3}Ba_{1/3}Mn_{1-x}Fe_xO_3$ manganites series.

4. Discussion

The observed reductions of M_s and T_c with Fe concentration are consistent with the incorporation of Fe atoms into the crystal structure of the $La_{2/3}Ba_{1/3}Mn_{1-x}Fe_xO_3$ manganites series, since both magnetic properties, being of intrinsic character, are highly sensitive to the chemical composition. The progressive incorporation of Fe^{3+} atoms into the unit cell of our LaBa-based manganites strongly influences their Mn^{4+}/Mn^{3+} ratio, which in turn plays a decisive influence on their electronic properties through mobile holes and the associated double exchange (DE) mechanism. The marked reduction observed for M_s and T_c as a function of the Fe content can be attributed to the weakening of the DE interaction between Mn^{3+} and Mn^{4+} pairs as follows: according to Ahn et al. [19], there is a poor overlap between the e_g bands of Mn^{3+} and Fe^{3+} and hence, electron hopping from Mn to Fe cations is energetically hindered. Therefore, the DE coupling is progressively deteriorated as the Fe content increases. The valence state of the Fe^{3+} cations within the perovskite structure has been confirmed by means of Mössbauer spectroscopy in similar $LaSr(MnFe)O_3$ manganites [20]. In addition, the replacement of Mn by Fe cations provokes also a reduction of the Mn^{3+}/Mn^{4+} ratio, thus producing a depopulation of the e_g band (which contains hoping electrons), together with a diminishing number of available hopping sites, since Fe^{3+} (with configuration $[Ar]3d^5$) has no empty site available for a hopping process preserving parallel spin alignment. In consequence, DE interaction is progressively suppressed as the Fe content increases.

5. Conclusions

The Pechini method is an effective route to obtain LaBa-based manganites with partial substitutions of Mn by Fe. Magnetic properties exhibited a marked dependence with the incorporation

of Fe atoms into the crystal structure, together with interesting magnetocaloric values of up to -1.46 J/kgK for $\Delta H = 2.5$ T, which represents an enhanced property when compared with equivalent LaSr-based manganites with same Mn/Fe replacement.

Acknowledgment

I. Betancourt acknowledges financial support from research Grant UNAM-PAPIIT IN104310, as well as the valuable technical assistance of Adriana Tejeda and Omar Novelo (both from IIM-UNAM) for XRD and SEM measurements, respectively.

References

[1] Y. Tokura, Rep. Prog. Phys. 69 (2006) 797–851.
[2] J.B. Goodenough, Rep. Prog. Phys. 67 (2004) 1915–1993.
[3] Manh-Huong Phan, Seong-Cho Yu, J. Magn. Magn. Mater. 308 (2007) 325–340.
[4] J. Paul Attfield, Chem. Mater. 10 (1998) 3239–3248.
[5] A.J. Millis, Nature 392 (1998) 147–150.
[6] A. Urushibara, Y. Moritomo, T. Arima, A. Asamitsu, G. Kido, Y. Tokura, Phys. Rev. B 51 (1995) 14103.
[7] C. Chu, T. Li, H. Wang, J. Wang, Physica B 405 (2010) 4523–4525.
[8] M. Koubaa, W. Cheikh-Rouhou Koubaa, A. Cheikhrouhou, J. Alloy. Compd. 479 (2009) 65–70.
[9] Y. Cui, R. Wang, L. Zhang, J. Appl. Phys. 103 (2008) 073907.
[10] S. Das, D. Dhak, M.S. Reis, V.S. Amaral, T.K. Dey, Mater. Chem. Phys. 120 (2010) 468–471.
[11] J. Wang, W. Wang, Y. Lei, F. Qin, J. Magn. Magn. Mater. 322 (2010) 1884–1888.
[12] H.L. Ju, J. Gopalakrishnan, J.L. Peng, Q. Li, G.C. Xiong, T. Venkatesan, R.L. Greene, Phys. Rev. B 51 (1995) 6143–6146.
[13] A.M. Tishin, Y.E. Spichkin, The Magnetocaloric Effect and its Applications, Institute of Physics, Bristol-Philadelphia, 2003.
[14] J. Zhang, H. Tanaka, T. Kanki, J.H. Choi, T. Kawai, Phys. Rev. B 64 (2001) 184404.
[15] M.P. Pechini, U.S. Patents No. 3330697, 11 July 1967.
[16] Y.J. Kwon, J. Ceram. Process. Res. 3 (2002) 146.
[17] Lone-Wen Tai, Paul A. Lessing, J. Mater. Res. 7 (1992) 511.
[18] S.K. Barik, C. Krishnamoorthi, R. Mahendiran, J. Magn. Magn. Mater. 323 (2011) 1015.
[19] K.H. Ahn, X.W. Wu, K. Liu, C.L. Chien, Phys. Rev. B 54 (1996) 15299.
[20] G. Zhang, J. Lin, J. Alloy. Compd. 507 (2010) 47.